Introduction to Quantum Chromodynamics

Michal Šumbera

Nuclear Physics Institute ASCR, Prague

December 15, 2009

Literature

Our discussion is based on

Quarks, partons and Quantum Chromodynamics

by Jiří Chýla

Available at http://www-hep.fzu.cz/ chyla/lectures/text.pdf

Introduction

- Previous lecture: discussed the problems resulting from singular behavior at *short distances* and outlined the remedy to these problems: the renormalization procedure.

- This lecture: analyses problems of gauge theories with massless gauge particles at *long distances*.

- Associated infinities emerge from theoretical considerations on the level of partons and reflects experimental restrictions by the finite resolution power. This naturally leads to the concept of **jet**.

- We address the question concerning relation of *partonic jets* to experimentally defined *jets of hadrons*. This is crucial for many applications of QCD to hard scattering processes and will be illustrated on the simplest example of three jet production in $\mathrm{e}^+\mathrm{e}^-$ annihilations.

Mass singularities in perturbation theory

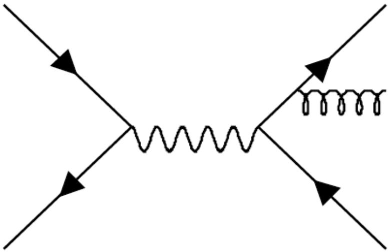

Figure 1: $e^+e^- \to \mathrm{q\overline{q}G}$

- Consider $$\mathrm{e^+e^- \to q\overline{q}G}, \qquad (1)$$ where gluon G is radiated either from q or $\mathrm{\overline{q}}$ (Fig. 1).
- Spin and color averaged cross section of (1) depends on two of the three dimensionless fractions x_i ($E_i, i = 1, 2, 3$ are the CMS energies of $\mathrm{q}, \mathrm{\overline{q}}$ and G, respectively)

$$0 \le x_i \equiv \frac{2E_i}{\sqrt{s}} \le 1; \quad \sqrt{s} = E_1 + E_2 + E_3 \Rightarrow x_1 + x_2 + x_3 = 2, \qquad (2)$$

or, equivalently, on three scaled invariant masses y_{ij} of of two partons:

$$y_{12} \equiv \frac{(p_1 + p_2)^2}{s} = 1 - x_3; \quad y_{13} \equiv \frac{(p_1 + p_3)^2}{s} = 1 - x_2; \quad y_{23} \equiv \frac{(p_2 + p_3)^2}{s} = 1 - x_1, \qquad (3)$$

for which the kinematical constraint in (2) implies $y_{12} + y_{13} + y_{23} = 1$.

Mass singularities in perturbation theory

- For *massless* quarks and gluons

$$\frac{\mathrm{d}\sigma}{\mathrm{d}x_1\mathrm{d}x_2} = \sigma_0 \frac{\alpha_s}{2\pi} C_F \frac{x_1^2 + x_2^2}{(1-x_1)(1-x_2)} \Leftrightarrow \frac{\mathrm{d}\sigma}{\mathrm{d}y_{13}\mathrm{d}y_{23}} = \sigma_0 \frac{\alpha_s}{2\pi} C_F \frac{(1-y_{23})^2 + (1-y_{13})^2}{y_{13}y_{23}}, \tag{4}$$

  where $C_F = 4/3$ and $\sigma_0 = 12\pi\alpha^2 e_q^2/3s$ is Born cross–section for production of a $\mathrm{q}\overline{\mathrm{q}}$ pair with electric charge e_q and three colors.

- Singularity at $x_1 = 1$ (i.e. at $y_{23} = 0$) corresponds to $G \| \overline{\mathrm{q}}$, while that at $x_2 = 1$ occurs when $G \| q$. Double singularity at $x_1 = x_2 = 1$ (i.e. at $x_3 = 0$) corresponds to the case when energy of the emitted gluon vanishes.

- Using $Q^2 \equiv m_{\overline{q}G} = s(1-x_1)$, in the collinear limit $x_1 \to 1$, which is equivalent to $Q^2/s \to 0$:

$$\frac{\mathrm{d}\sigma}{\mathrm{d}Q^2\mathrm{d}x_2} = \frac{1}{s}\frac{\mathrm{d}\sigma}{\mathrm{d}x_1\mathrm{d}x_2} = \sigma_0 \frac{\alpha_s}{2\pi}\frac{1}{Q^2} C_F \frac{x_1^2 + x_2^2}{1-x_2}$$

$$\underset{x_1 \to 1}{\longrightarrow} \quad \sigma_0 \frac{\alpha_s}{2\pi}\frac{1}{Q^2} C_F \frac{1+x_2^2}{1-x_2} = \sigma_0 \frac{\alpha_s}{2\pi}\frac{1}{Q^2} P_{qq}^{(0)}(x_2). \tag{5}$$

- N.B. in the collinear limit $x_1 \to 1$ the variable x_2 represents a fraction of the momentum of the original $\overline{\mathrm{q}}$ carried by it after the emission of G.
- Available kinematical region covers interior of the triangle in Fig. 2a, with bands defining the regions where one of the y_{ij} is small. Fig. 2b shows the typical configurations corresponding to these three regions.
- When the $\mathrm{q}\overline{\mathrm{q}}$ pair is close in phase space, the cross–section is *not* singular. This is illustrated in Fig. 2c, where a scatterplot corresponding to the cross–section (4) is displayed.

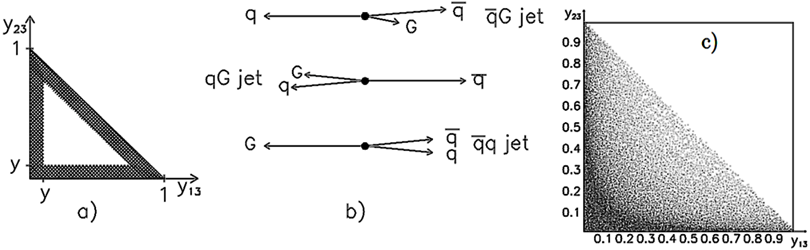

Figure 2: Kinematics of $\mathrm{q}\overline{\mathrm{q}}$G final state (a), typical configurations corresponding to qG or $\overline{\mathrm{q}}$G jets (b) and scatterplot of events generated according to (4).

Mass singularities in perturbation theory

- Introducing $\beta \equiv m_g^2/Q^2$, and assuming $\beta \neq 0$ cross-section for (1) reads:

$$\frac{\mathrm{d}\sigma}{\mathrm{d}x_1\mathrm{d}x_2} = \sigma_0 \frac{2\alpha_s}{3\pi} \frac{1}{(1-x_1)(1-x_2)} \times$$

$$\left[x_1^2 + x_2^2 + \beta\left(2(x_1+x_2) - \frac{(1-x_1)^2 + (1-x_2)^2}{(1-x_1)(1-x_2)}\right) + 2\beta^2\right]. \qquad (6)$$

- The singularities, both infrared and parallel, are screened off. Kinematical bounds on x_1, x_2 are now functions of β:

$$0 \leq x_1 \leq 1-\beta; \quad 1-\beta-x_1 \leq x_2 \leq 1 - \frac{\beta}{1-x_1}. \qquad (7)$$

- (6) is symmetric in x_1, x_2. Integration over one of these fractions yields:

$$\frac{\mathrm{d}\sigma}{\mathrm{d}x} = \sigma_0 \frac{\alpha_s}{2\pi}\frac{4}{3} \times \qquad (8)$$

$$\times\left[\frac{1+x^2}{1-x}\ln\frac{x(1-x)}{\beta} - \frac{3}{2}\frac{1}{1-x} + \frac{1}{2}(x+1) + \beta\frac{2-x}{(1-x)^2} + \frac{1}{2}\beta^2\frac{1}{(1-x)^3}\right]$$

where $0 \leq x \leq 1-\beta$ and only terms contributing when $\beta \to 0$ were retained.

Mass singularities in perturbation theory: virtual gluon

- N.B. Contrary to the double differential cross–section (6), which has a meaning even for $\beta = 0$, expression (8) blows to infinity for $\beta \to 0$.
- Instead of radiating a *real* gluon, the quark can radiate a *virtual* one (G^*), which will eventually recombine with an accompanying antiquark (Fig. 3 left) or producing a real $q\overline{q}$ pair (Fig. 3 right), with the parent quark.
- In both cases G^* can be arbitrarily close to its mass-shell and thus propagate to arbitrarily large distances.

⇒ Integration over the loops of Fig. 3 leads also to mass singularities.

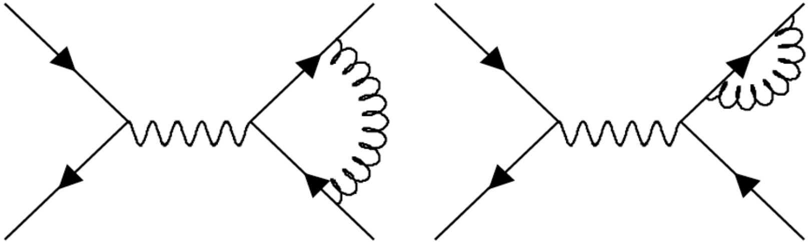

Figure 3: Virtual gluon emission in $e^+e^- \to q\overline{q}$.

Mass singularities in perturbation theory: virtual gluon

- Interference term between the lowest order QPM diagram and loop diagrams in Fig. 3 is of the same order α_s as the square of the diagram in Fig. 1, describing the real gluon emission

$$\sigma_{\rm virt} = \sigma_0 \frac{\alpha_s}{2\pi}\frac{4}{3}\left[-\ln^2\beta - 3\ln\beta + \frac{\pi^2}{3} - \frac{7}{2}\right] + \mathcal{O}(\alpha_s^2). \tag{9}$$

- This term contributes obviously only for $x = 1$ and we can write

$$\frac{{\rm d}\sigma_{\rm virt}}{{\rm d}x} = \sigma_0 \frac{\alpha_s}{2\pi}\frac{4}{3}\left[-\ln^2\beta - 3\ln\beta + \frac{\pi^2}{3} - \frac{7}{2}\right]\delta(1-x). \tag{10}$$

⇒ Crucial observation: gluon with zero energy is the same as no gluon at all. *For massless gluons we can add the $-\infty$ from virtual correction to the cross section $\sigma(e^+e^- \to {\rm q\bar{q}})$ to $+\infty$ coming from the integral over the real gluon emission*.

- N.B. To carry out this cancelation in a mathematically well-defined way, the regulator $\beta \neq 0$ was introduced.

Mass singularities in perturbation theory

To work out this sum, several rather technical steps have to be carried out:

1. Although the last two terms in (8) are proportional to β and β^2, they *cannot* be neglected in the limit $\beta \to 0$. Their limit is $\frac{5}{4}\delta(1-x)$.

2. Realizing that $$\delta(1-x) = \delta(1-x-\beta) + \beta\delta^{'}(1-x) \qquad (11)$$

   and taking into account that in (10) the dependence on β comes only in powers of $\ln\beta$, we can replace $\delta(1-x)$ in (10) with $\delta(1-x-\beta)$.

3. We now recall the definition of the so called "+" distribution

   $$[f(x)]_+ \equiv \lim_{\beta\to 0}\left(f(x)\theta(1-x-\beta) - \delta(1-x-\beta)\int_0^{1-\beta} f(y)\mathrm{d}y\right), \qquad (12)$$

   where $\theta(x)$ is usual step function. For functions singular at $x=1$ the second term subtracts at $x=1$ the whole (possibly divergent) integral over this interval.

We shall need the following explicit results

$$\left[\frac{1}{1-x}\right]_+ = \frac{1}{1-x}\theta(1-x-\beta) + \ln\beta\,\delta(1-x-\beta), \qquad \left[\frac{1+x^2}{1-x}\right]_+ = \frac{1+x^2}{[1-x]_+} + \frac{3}{2}\delta(1-x)$$

$$\frac{1+x^2}{[1-x]_+} = \frac{1+x^2}{1-x}\theta(1-x-\beta) + 2\ln\beta\,\delta(1-x-\beta), \tag{13}$$

$$(1+x^2)\left[\frac{\ln(1-x)}{1-x}\right]_+ = \frac{(1+x^2)\ln(1-x)}{1-x}\theta(1-x-\beta) + 2\ln^2\beta\,\delta(1-x-\beta)$$

4. Regroup individual terms in the sum of (8) and (10) in such a way that the limit $\beta \to 0$ can be carried out to get:

$$\frac{\mathrm{d}\sigma}{\mathrm{d}x} \equiv \frac{\mathrm{d}\sigma_{\mathrm{real}}}{\mathrm{d}x} + \frac{\mathrm{d}\sigma_{\mathrm{virt}}}{\mathrm{d}x} = \sigma_0 \frac{\alpha_s}{2\pi}\frac{4}{3}\left\{ \ln\frac{1}{\beta}\left[\frac{1+x^2}{1-x}\right]_+ + \right. \tag{14}$$

$$\left. \underbrace{(1+x^2)\left[\frac{\ln(1-x)}{1-x}\right]_+ + \frac{1+x^2}{1-x}\ln x - \frac{3}{2}\frac{1}{[1-x]_+} + \frac{1+x}{2} + \left(\frac{\pi^2}{3} - \frac{9}{4}\right)\delta(1-x)}_{\text{constant terms}} \right\}.$$

Mass singularities in perturbation theory

5. Finally, integrating (14) over x we get

$$\sigma_{\rm tot} \equiv \sigma_{\rm real} + \sigma_{\rm virt} = \sigma_0 \frac{\alpha_s}{\pi}. \quad (15)$$

We could get the last result also by adding the integral of (6), equal to

$$\sigma_{\rm real}(Q) = \sigma_0 \frac{\alpha_s}{2\pi} \frac{4}{3} \left[\ln^2\beta + 3\ln\beta - \frac{\pi^2}{3} + 5 \right], \quad (16)$$

to (9) and sending $\beta \to 0$.

- Terms $\propto \ln\beta$ come from parallel as well as IR region of gluon momenta, while the double logarithm $\ln^2\beta$ comes entirely from the IR region.
- In both cases the virtuality of q or $\overline{\mathrm{q}}$ emitting G is $\propto m_g^2$ and thus vanishes with it. Physically it means that virtual q or $\overline{\mathrm{q}}$ propagate to distances of the order $1/m_g$ before radiating G and going to their mass shell.
- Remarkably, if we add the real and virtual gluon emission cross-sections we get a *finite* result for the total cross–section (15) and a well–defined expression for the inclusive spectrum (14).

Kinoshita–Lee–Nauenberg theorem

Consider the general scattering process $A \to B$ between states A, B of massive particles. It may happen that the scattering matrix $|S_{AB}|$ has mass singularities but if we sum the squares of scattering amplitudes

$$\sum_{D(A),D(B)} \left|S_{D(A)D(B)}\right|^2 \qquad (17)$$

over the sets $D(A), D(B)$ of states degenerate with A,B, the sum has no mass singularities, i.e. is finite even for massless particles.

- Here "degenerate" = all states of particles having the same conserving quantum numbers as well as the same total four–monentum. Degenerate states thus may have different number and composition of particles.
- In QED the states of an electron and an electron accompanied by a photon with zero energy are degenerate. However, even a 10 GeV electron and a *parallel* pair of a 5 GeV electron with a 5 GeV photon would be degenerate in the limit of vanishing electron mass.
- KLN is useful when ΔE or Δp_T resolution $\delta \gg m_e$. Setting $m_e = 0$ we can safely invoke KLN theorem to calculate σ for particular process with or without additional γ with $E_\gamma > \delta$.

Application of KLN theorem to DIS

- Lowest order QCD corrections to QPM in DIS: one gluon emission from incoming or outgoing quarks (Fig. 4a). Similarly to $\mathrm{e^+e^- \to q\bar{q}G}$, soft and parallel singularities appear when integrating over energies and angles of the emitted G.

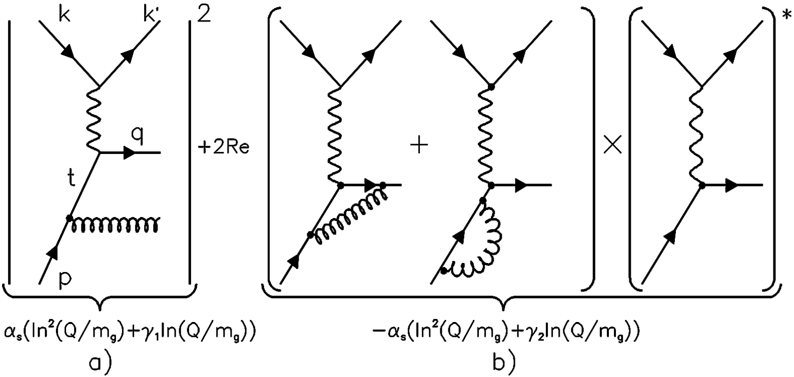

Figure 4: Application of KLN to DIS. t in a) denotes virtuality of intermediate quark. Double logarithms, coming from the soft gluon emission, cancel in sum of real and virtual contributions, while single logarithms do not and give the term $\ln(1/\beta)$ in (14).

Application of KLN theorem to DIS

- Regulation of singularities via m_g leads again to $\propto \ln\beta, \ln^2\beta$ as in (16).
- Keeping $x \equiv -q^2/2pq$ and $y \equiv (qp)/(kp)$ fixed, but integrating over all other variables describing the quark level subprocess $\mathrm{e}+\mathrm{q}\to\mathrm{e}+\mathrm{q}+\mathrm{G}$, we find that diagram in Fig. 4a contributes

$$\frac{\mathrm{d}\sigma^{\mathrm{real}}}{\mathrm{d}x\mathrm{d}y} = \left[\frac{4\pi\alpha^2 xs}{Q^4}\frac{1+(1-y)^2}{2}\right]\frac{\alpha_s}{\pi}\left(\frac{4}{3}\frac{1+x^2}{1-x}\ln\frac{1}{\beta}+f(x,\beta)\right), \quad (18)$$

  where $s=(k+p)^2$ and x is the fraction of incoming quark momentum, carried by it after the gluon emission. Function $f(x,\beta)$ has a *finite* limit for $\beta\to 0$. Singular term proportional to $\ln 1/\beta$, results, as in (14), from integration over the angle of the emitted gluon.

- Interference between diagrams in Fig. 4b contributes again a negative divergent term

$$\frac{\mathrm{d}\sigma^{\mathrm{virt}}}{\mathrm{d}x\mathrm{d}y} = \left[\frac{4\pi\alpha^2 xs}{Q^4}\frac{1+(1-y)^2}{2}\right]\frac{4\alpha_s}{3\pi}\left(-\ln^2\beta-3\ln\beta-\frac{7}{2}-\frac{2\pi^2}{3}\right)\delta(1-x) \quad (19)$$

  and $\delta(1-x)$ expresses the fact that G^* emission contributes only for $x=1$.

- Adding the above two contributions involves the same kind of manipulations as for the process (1) and leads to the following result

$$\frac{\mathrm{d}\sigma_{\mathrm{real}}}{\mathrm{d}x\mathrm{d}y}+\frac{\mathrm{d}\sigma_{\mathrm{virt}}}{\mathrm{d}x\mathrm{d}y}=\left[\frac{4\pi\alpha^2 xs}{Q^4}\frac{1+(1-y)^2}{2}\right]\left(\frac{\alpha_s}{\pi}\underbrace{\frac{4}{3}\left[\frac{1+x^2}{1-x}\right]_+}_{P_{qq}^{(0)}(x)}\ln\frac{1}{\beta}+f(x,\beta)\right) \quad (20)$$

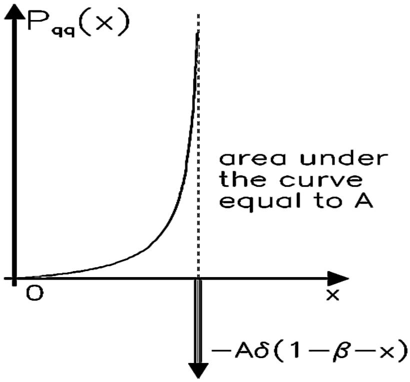

Figure 5: Branching function $P_{qq}(z)$.

- Shape of $P_{qq}^{(0)}(z)$ is sketched in Fig. 5. This so called *Altarelli–Parisi "splitting function"* has the important property

$$\int_0^1 P_{qq}^{(0)}(z)\mathrm{d}z=0, \quad (21)$$

which is a straightforward consequence of the definition (12). Physical interpretation of this relation will be later on.

Introduction into the theory of jets

- State with $|\, N_G \neq 0, E_G = 0\rangle \equiv |\, N_G = 0\rangle$,
  but state $|\, N_G \neq 0, E_G \geq \varepsilon > 0\rangle \neq |\, N_G = 0\rangle$ however small ε might be.

$\Rightarrow$ Theoretically meaningful and experimentally answerable question:
What is $\sigma_{3\mathrm{parton}}(y)$ in the kinematical region outside the singularity, for instance for $y_{ij} \geq y$, where the cut–off parameter $y > 0$ defines this region?

- Complementary, question: What's $\sigma_{q\bar{q}}(y)$ or $\sigma_{q\bar{q}G}(y)$ for $y > y_{13}$ or $y > y_{23}$? Integral over this region *always* contains also the contribution from the virtual corrections to the $\mathrm{q\bar{q}}$ final state and therefore *decreases* as $y \to 0$.

- In this ways we are naturally led to *y–dependent definition of the* **jet**:
  At the order α_s jet is simply either a single parton or a pair of partons (i, j) with the scaled invariant mass satisfying $y_{ij} \leq y$.

- **Physically measurable** *two–jet final state*: either a $\mathrm{q\bar{q}}$ pair or $\mathrm{q\bar{q}G}$ final state, in which the gluon is close to either q or $\mathrm{\bar{q}}$. In the latter case the jet momentum is defined as the vector sum $p_{\mathrm{jet}} \equiv p_i + p_j$ of the pair (i, j).

Theory of jets: dimensional regularization

- To the order α_s and in $n = 4 - 2\varepsilon$ dimensions, the contribution to 2–jet cross–section coming from $\mathrm{q\overline{q}}$ final state reads:

$$\sigma_{2\mathrm{jet}}(q\overline{q}) = \frac{\sigma^{(2)}}{1-\varepsilon}\left[1 - \varepsilon + C_F \frac{\alpha_s(\mu)}{2\pi}\left(\frac{4\pi\mu^2}{Q^2}\right)^{\varepsilon} A_1 + \mathcal{O}(\alpha_s^2)\right], \qquad (22)$$

where

$$\sigma^{(2)} \equiv \left(\frac{4\pi\mu^2}{Q^2}\right)^{\varepsilon} \frac{\Gamma(2-\varepsilon)}{\Gamma(2-2\varepsilon)}\sigma_0, \quad \sigma_0 \equiv \frac{4\pi\alpha^2}{3Q^2}\left(3\sum_f e_f^2\right), \qquad (23)$$

is the Born cross–section for $\mathrm{e^+e^-}$ annihilation into a $\mathrm{q\overline{q}}$ pair in n dimension, $\zeta_2 \equiv \pi^2/6$ and the contribution from virtual corrections is determined by the coefficient

$$A_1 = \frac{\Gamma(1+\varepsilon)\Gamma^2(1-\varepsilon)}{\Gamma(1-2\varepsilon)}\left(-\frac{2}{\varepsilon^2} - \frac{1}{\varepsilon} + 6\zeta_2 - 5 + 3\zeta_2\varepsilon - 8\varepsilon\right). \qquad (24)$$

where $\zeta_2 = \pi^2/3$.

- Note that ε can be sent to zero everywhere except A_1 and that the cut–off parameter y is absent from (22).

Theory of jets: dimensional regularization

- Integrating the cross–section corresponding to the $\mathrm{q\overline{q}G}$ final state over the region $y_{ij} \leq y$ we get

$$\sigma_{\mathrm{2jet}}(q\overline{q}G) = \frac{\sigma^{(2)}}{1-\varepsilon}\left[C_F \frac{\alpha_s(\mu)}{2\pi}\left(\frac{4\pi\mu^2}{Q^2}\right)^{\varepsilon} B_1 + \mathcal{O}(\alpha_s^2)\right], \tag{25}$$

where

$$B_1 = \frac{\Gamma(1+\varepsilon)\Gamma^2(1-\varepsilon)}{\Gamma(1-2\varepsilon)}\left(\frac{2}{\varepsilon^2} + \frac{1}{\varepsilon} + 4 - 4\zeta_2 - 3\ln y - 2\ln^2 y\right). \tag{26}$$

- Comparing (22) and (25) we see that the singular terms $1/\varepsilon^2$ and $1/\varepsilon$ enter A_1 and B_1 with *opposite* signs and thus *cancel* in the physical 2–jet cross–section σ_{2jet}, given as their sum:

$$\sigma_{\mathrm{2jet}}(y) = \sigma_0\left[1 + \frac{\alpha_s}{2\pi} C_F\left(-2\ln^2 y - 3\ln y + 2\zeta_2 - 1\right) + \mathcal{O}(\alpha_s^2)\right]. \tag{27}$$

- The $\mathcal{O}(\alpha_s)$ 3–jet cross–section, resulting from integration of (25) in the complementary region $y_{ij} > y$ equals

$$\sigma_{\mathrm{3jet}}(y) = \sigma_0\left[\frac{\alpha_s}{2\pi} C_F\left(2\ln^2 y + 3\ln y - 2\zeta_2 + 5/2\right) + \mathcal{O}(\alpha_s^2)\right]. \tag{28}$$

Jet rates

- Note the different character of the y dependence in (27) compared to (28): while $\sigma_{2\text{jet}}(y)$ is a decreasing function of y it is vice versa for $\sigma_{3\text{jet}}(y)$! Smaller is y more gluon radiation is "resolved" and counted as 3–jet final state.

- Summing $\sigma_{2\text{jet}}$ and $\sigma_{2\text{jet}}$ we get $\sigma_{\text{tot}}^{(2)} \equiv \sigma_0(1 + \alpha_s/\pi)$, the total cross–section of $\mathrm{e^+e^-}$ annihilation to partons at the order $\mathcal{O}(\alpha_s)$, which by construction is y–independent.

- **Jet rates** $R_i \equiv \sigma_{i\text{jet}}(y)/\sigma_0(1 + \alpha_s/\pi)$ for $i = 2, 3$ are plotted in the left panel of Fig. 7.

- $R_i, i = 2, 3, 4$ measured by OPAL experiment at LEP are shown in the right panel of Fig. 7. As y decreases more and more jets pop up, their cross–section first rapidly increasing, peaking at some y and finally decreasing to make place for even more jets. Quantitative comparison of these data with theoretical predictions is, however, more complicated.

Jet rates

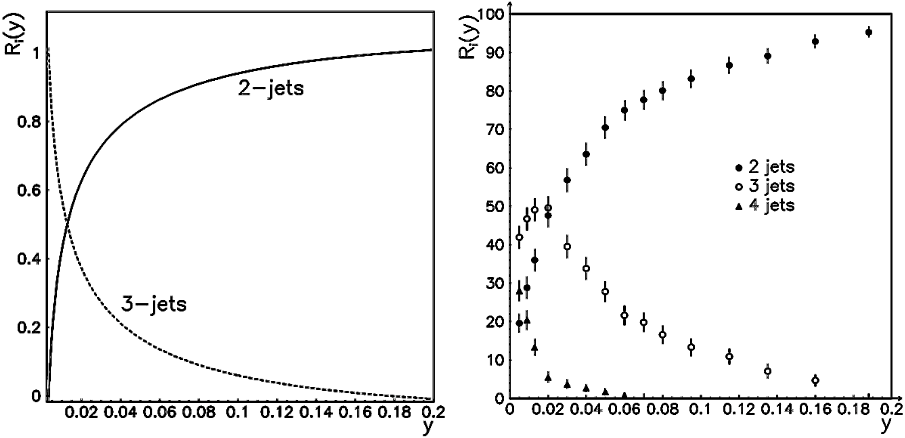

Figure 6: Left: two and three jet rates $R_i(y)$ according to formulae (27) and (28). Right: experimental data on 2–4 jet rates in $\mathrm{e}^+\mathrm{e}^-$ annihilations as measured by the OPAL Collaboration at LEP.

Jet algorithms

Definition of jets in e^+e^- annihilations into 2 or 3 final state partons the is simple and almost unambiguous. Situation is more complicated if

- more partons in final states are taken into account,
- other process (like hadron–hadron or electron–proton collisions) are analyzed,
- consistency of theoretical definition of jet is to be guaranteed,
- jet definition should be applicable to observable hadrons as well.

For multi-parton final states there are two different ways how to define jets.

Jet algorithms: Clustering

- Repeated combining of two massless partons into one, again massless, parton.
- We *cannot* simply add parton four–momenta (for noncollinear pairs this would inevitably result in a nonzero mass of the recombined pair).

⇒ Either sum three–momenta and adjust energy (thus violating energy conservation) or sum energies and adjust longitudinal momentum of the pair (thus violating its conservation).

- Distance of partons is given by $y_{ij} \equiv 2E_iE_j(1 - \cos\theta_{ij})/Q^2$.
- Recipe: Start with any parton, recombine it with its nearest neighbourgh in $y_{ij} \Leftrightarrow y_{ij} \leq y$ and proceed untill all the remaining pairs have $y_{ij} > y$. This defines the so called **JADE** algorithm.
- A closely related, but theoretically superior, is the so called **Durham** jet algorithm, which replaces m_{ij} with the "transverse" distance $d_{ij} \equiv 2\min(E_i^2, E_j^2)(1 - \cos\theta_{ij})$.

The cone algorithm

Second approach looks for *groups of partons that are within given "distance" from their "center"*. The relevant distance can be defined in various ways.

- In **Sterman–Weinberg cone** jet algorithm angular separation defines this distance. Jet momentum and energy are then given as sums of momenta and energies of all particles that lie with a given angle θ from their center. E_{jet} therefore has to exceed certain minimal value ϵ.
- For **CDF cone** jet algorithm the "distance" is defined by the variable

$$R \equiv \sqrt{(\Delta\eta)^2 + (\Delta\phi)^2}, \quad \eta \equiv -\ln(\tan\theta/2), \tag{29}$$

where ϕ is the azimuthal angle. E_T, η and ϕ of the jets are given as:

$$E_T^{\mathrm{jet}} \equiv \sum_i E_T^i, \qquad \eta^{\mathrm{jet}} \equiv \sum_i \frac{E_T^i}{E_T^{\mathrm{jet}}}\eta^i, \qquad \phi^{\mathrm{jet}} \equiv \sum_i \frac{E_T^i}{E_T^{\mathrm{jet}}}\phi^i, \tag{30}$$

sum running over all particles within the jet.

For different processes different algorithms are theoretically preferable. JADE algorithm was originally developed for $\mathrm{e}^+\mathrm{e}^-$ and is still being used there. In $\ell + h$ and $h + h$ collisions CDF cone algorithm is theoretically superior.

Jets of partons vs jets of hadrons

Hadrons, not partons, are observed in experiment.

- Rule of thumb: *Higher p_T of the jets, smaller is the differences between properties of partonic and hadronic jets*.
- For a given value of jet resolution parameter y we can be evaluated theoretically $\mathrm{d}\sigma^{\mathrm{theor}}/\mathrm{d}p_T$. Experimentalist can do the same with hadrons and thus measure $\mathrm{d}\sigma^{\mathrm{exp}}/\mathrm{d}p_T$. Should we compare these two distributions for the same y, or not? And under which conditions can we do it?
- The only way out is to construct some **models** of hadronization (recall independent fragmentation model), study this relation within each model separately and then compare the corresponding results among as many hadronization models as possible.
- An alternative way is to include as much as possible of the theoretical calculations at the level of partons within the so called **event generators**, Monte Carlo programs that mix perturbative QCD calculation of partonic collisions with models of hadronizations. In this case experimental jets are compared not with partonic jets but also with hadronic jets, simulated within these event generators.

Jets of partons vs jets of hadrons

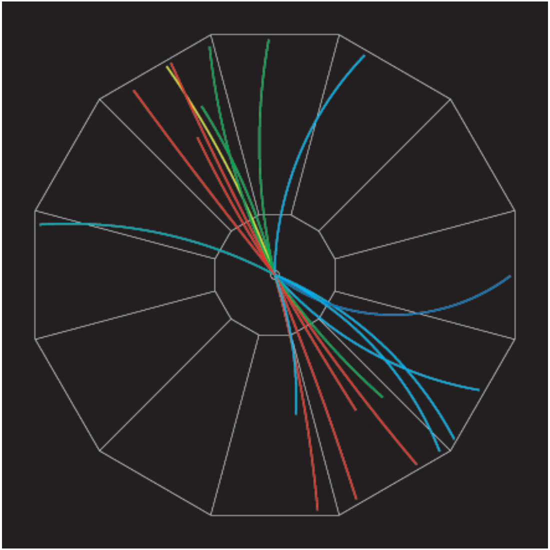

Figure 7: Jets of (charged) hadron from p+p collisions at $\sqrt{s} = 200\text{GeV}$ as seen in by STAR experiment at RHIC.

Exercises

1. Calculate explicitly (4), (6).
2. Derive the kinematical bounds (7).
3. Prove that for quite general $f(z)$ the definition of "+" distribution as given in (12) is equivalent to the following one

$$\int_0^1 [f(z)]_+ g(z)\mathrm{d}z \equiv \int_0^1 f(z)(g(z) - g(1))\mathrm{d}z.$$

4. Show that from definition

$$\int_0^1 [f(z)]_+ = 0.$$